DOI:
10.1021/jacs.8b09086

Control over Near-Ballistic Electron Transport through Formation of Parallel Pathways in a Single-Molecule Wire

Albert C. Aragonès,[†v] Nadim Darwish,[#] Simone Ciampi,[#] Li Jiang,[‡] Raphael Roesch,[|] Eliseo Ruiz,[*^v] Christian A. Nijhuis[*‡Δ] and Ismael Díez-Pérez [*†]

[†] Department of Chemistry, Faculty of Natural & Mathematical Sciences, King's College London, Britannia House, 7 Trinity Street, London SE1 1DB, United Kingdom.

[v] Institut de Química Teòrica i Computacional (IQTC), Universitat de Barcelona, Diagonal 645, 08028 Barcelona.

[^] Departament de Química Inorgànica i Orgànica, Universitat de Barcelona, Diagonal 645, 08028 Barcelona, Spain.

[#] School of Molecular and Life Sciences, Curtin University, Bentley WA 6102, Australia.BF

[‡] Department of Chemistry, National University of Singapore, 3 Science Drive 3, Singapore 117543.

[Δ] Centre for Advanced 2D Materials, National University of Singapore, 6 Science Drive 2, Singapore 117546.

[|] Center for Biosensors and Bioelectronics, Biodesign Institute, Arizona State University, Tempe, Arizona 85287, USA.

Abstract:

This paper reports highly efficient coherent tunneling in single-molecule wires of oligo-ferrocenes with one to three Fc units. The Fc units were directly coupled to the electrodes, *i.e.* without chemical anchoring groups between the Fc units and the terminal electrodes. We found that a single Fc unit readily interacts with the metal electrodes of an STM-break junction (STM = scanning tunneling microscope) and that the zero-voltage bias conductance of an individual Fc molecular junction increased 5-fold, up to 80% of the conductance quantum G_o (77.4 μS), when the length of the molecular wire was increased from one to three connected Fc units. Our compendium of experimental evidences combined with non-equilibrium Green functions calculations contemplate a plausible scenario to explain the exceedingly high measured conductance based on the electrode/molecule contact via multiple Fc units. The oligo-Fc backbone is initially connected through all Fc units and, as one of the junction electrodes is pulled away, each Fc unit is sequentially disconnected from one of the junction terminals resulting in several distinct conductance features proportional to the number of Fc units in the backbone. The conductance values are independent of the applied temperature (-10 to 85°C), which indicates that the mechanism of charge transport is coherent tunneling for all measured configurations. These measurements show the direct Fc-electrode coupling provides highly efficient molecular conduits with very low barrier for electron tunneling, and whose conductivity can be modulated near the ballistic regime through the number of Fc units able to bridge and the energy position of the frontier molecular orbital.

Introduction

Molecular electronics consolidates as a research field that aims to complement traditional silicon integrated micro-circuits with molecular circuitry based on single molecules or self-assembled monolayers (SAMs).[1,2] Realizing molecular circuitries requires understanding the mechanisms of charge transport through metal-molecule-metal junctions, both experimentally and theoretically. Significant advances have been made towards understanding the fundamentals of the mechanisms of charge transport across junctions with single-molecules and SAMs in a very broad variety of molecular systems, reproducing a number of conventional electrical functionalities such as resistance,[3] transistor or diode effects,[4–8] in addition to fundamental studies of charge transport as a function of molecular length,[9–12] conjugation,[13–16] chemical substitutuents,[17–19] molecular conformation,[13,20–22] alignment of the molecular frontier orbitals to the electrode Fermi energy level,[23–26] aromaticity,[23,27] or anchoring group.[28–31] Most of these examples show conductance values of typically several orders of magnitudes below the conductance quantum G_0=77.4 µS, which evidences their resistive nature and their limitation as electron conduits in a molecular circuit.

Ferrocene (Fc) was the first example of a metallocene and it has been attractive in molecular electronics because of its good thermal and chemical stability and low-lying highest occupied molecular orbital (HOMO).[32–34] Fc binds weakly to the surface of common metals substrates such as Ag, Cu, Al, Mo or Au.[33,35–40] The Fc deposited on flat metal surfaces such as Ag (100), Cu (111) and Au (111) binds with the plane of the cyclopentadienyl moieties facing the surface.[33,36,41,42] These properties make Fc an attractive candidate in molecular electronics to provide simple electronic functions when properly linked to an electronic platform, including low resistivity and sharp gate-dependence,[43–46] or more complex operations such as negative differential resistance,[43,47] rectification[6,7,34,48] or Boolean logics.[7] A key parameter to achieve such large electrical tunability is the control over the Fc-electrode electronic coupling. Some applications require a weak Fc-electrode coupling to minimize the hybridization of the low-lying molecular orbital (here a HOMO), directly involved in the molecular charge transport, to the electrodes terminal[6,48]. Contrarily, a "high coupling" scenario could be designed by manipulating the delocalization of the low-lying HOMO level between several Fc units within the same molecular wire,[49,50] which, in turn, hybridizes to the device electrodes.[6,34] The latter is a much less studied case that could be exploited to build efficient molecular wires displaying high conductance G values close to G_0.[44,51]

Despite this tremendous progress in recent years, it is also well-known that molecules with the same chemical structure can yield molecular junctions with orders of magnitude differences in conductance depending on the fabrication technique that is used to construct the junctions.[52–54] Although the effective contact area among the different methods is largely responsible for this observation, the molecule-electrode interaction plays a crucial role. In large-area junctions, the electrodes are planar and therefore less reactive than the electrode generated in break junctions. In general, the former yields well-defined junctions that are usually resistive, while the latter yields highly conductive junctions with a wide range of possible geometries due to the dynamic way of collecting the molecular conductance.[55] Usually it is assumed that the electrodes only form a single contact with the molecules, however, the junction formation process might

involve the formation and rupture of multiple contact points depending upon the chemical nature of the studied molecular backbone.

Here, we present a study of single-molecule transport in STM break junctions of a new class of molecular wires composed of oligo-ferrocenes with one, two, and three directly connected ferrocene units, namely ferrocene (Fc), biferrocene (BFc) and 1-1'-terferrocene (TFc) (Fig. 1). The Fc units strongly interact with the terminal electrodes because of the high reactivity of uncoordinated gold atoms of the STM junction,[56] without the need for additional anchoring groups such as thiolates or amines.[28,31] We show that each individual Fc moiety within the molecular wire can readily form highly conducting junctions near the conductance quantum facilitating multiple Fc-electrode contacts with well-defined conductance signatures. During the rupture process, the contact points are broken one-by-one allowing us to control the number of contacts per molecule via the number of Fc units and STM tip displacement. This new conformation in a single-molecule junction can be used to interpret unexpectedly high G features observed in previous measurements incorporating Fc units.[44,46] All our findings are supported by extensive computational calculations and our observations give rise to new insights in the dynamics of the STM-break junction formation process. This work demonstrates Fc-oligomers are an interesting class of efficient nanoscale molecular wires displaying near ballistic transport and presents Fc as a new tunable molecule/electrode anchoring group with multiple contact points (through each individual Fc unit).

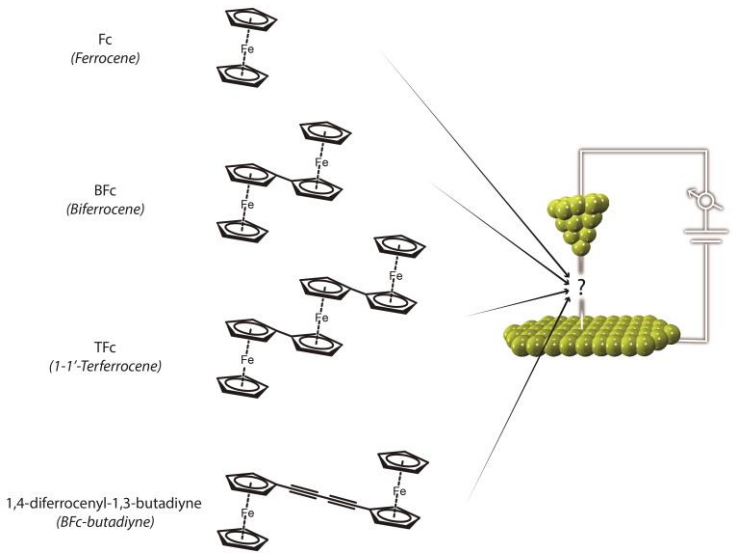

Fig. 1 Molecular structures of all studied oligo-ferrocenes in this work. We abbreviate ferrocene as Fc, biferrocene as BFc, terferrocene as TFc and 1,4-diferrocenyl-1,3-butadiyne as BFc-butadiyne.

Results and discussion

Conductance signatures of the single-molecule junctions

We measured the single-molecule conductance within a high conductance range near G_o (10^{-2} G_0 to $1G_0$) for the Fc, BFc, TFc and BFc-butadyine molecules (see details of the synthesis in the Supporting Information (SI) section 1) using the STM break-junction (STM-BJ) technique.

Technical details of the STM-BJ approach have been published elsewhere[3,23] (for more details see SI section 2). Briefly, a STM Au tip is firstly brought over a flat, clean Au(111) surface to a tunneling distance in a solution containing the molecule of interest. Then, the STM current feedback is turned off and the STM tip is repeatedly driven in and out of contact to and from the Au(111) surface. During the retraction stage, individual molecules that are either dissolved in the surrounding organic medium or adsorbed on the surface can be spontaneous trapped between the two electrodes. This pulling process is repeated thousands of times while the current is monitored, resulting in the collection of large amounts of current decay curves (4000–5000, see representative examples in Fig. 2 insets). Of these curves, 15-20% display plateau features corresponding to the quantum conductance of the single-molecule bridge.[57–59] Since not every current decay curve shows such plateau features, we designed an automatic algorithm that identifies and selects curves containing such single-molecule features. The exact same selection criteria were applied throughout all measured series (see more details in SI section 2). Conductance histograms were built by the accumulation of hundreds of selected individual current decays (displaying plateaus) and the resulting peak maxima represent the most probable conductance values of the studied single-molecule bridge. 1,2,4-Trichlorobenzene was employed as the solvent in all transport experiments (see SI sections 3 for more details and control experiments with different solvents).[60] It is worth noting from Figure 2 that each Fc unit establishes a well-defined contact geometry characterized by a single, symmetrical conductance signature (peak) as opposed to previously widely used anchoring chemistry that often result in multiple peaks, or shoulders and/or tails.[61–64]

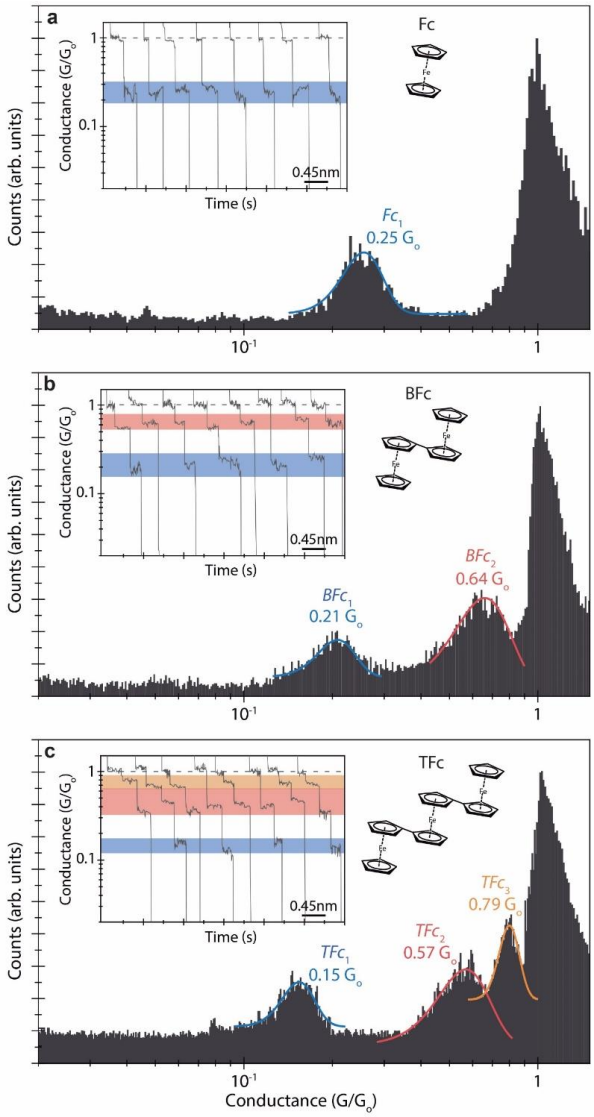

Fig. 2 Semi-log conductance histograms of the Fc **(a)**, BFc **(b)** and TFc **(c)** oligomers. Individual Gaussian fits of the peaks are used to extract the maxima values (indicated in the plot). The different molecular wire configurations are labelled as "(oligoFc)$_n$", being *n* the number of effectively bridged Fc units and the "oligo" term refereeing to Bi (B) or Ter (T). The insets show representative individual current traces displaying plateau features used to build the 1D histograms (2D maps accumulating all individual traces are shown in the SI section 4). The shadow coloured bands indicate the range of conductance for each plateau (line width extracted from the FWHM of the fitted histogram peaks). Counts have been normalized versus the total amount of counts. The applied voltage bias was set to 10 mV.

Sequentially disconnecting Fc units in the single-molecule junction

Figures 2a-c show a good correlation between the observed number of peaks within the studied high conductance range and the number of Fc units of the studied Fc-oligomer compound. A single plateau is always observed in the individual current decays for junctions with Fc (Fig. 2a), whereas junctions with BFc and TFc (Fig. 2b-c insets) shows that as the molecular junction is stretched (the Au STM tip electrode is pulled away from the Au surface), multiple plateaus concatenate with a good correlation in number to the number of existing Fc units in the backbone (Fig. 2a-c insets).[65,66] To analyze this correlation in detail, we plotted the data in a 2D

cross-correlation conductance map (see SI section 2 for additional details)[67,68]. Figure 3a shows the corresponding one for the molecular junction formed with the TFc, which is represented by a 2D histogram of the analyzed counts at a particular conductance value of the individual decay curve (Y-axis) against the full measured conductance range (X-axis). The appearance of the three red spots along both X and Y directions at the conductance values coincidental with the three conductance maxima (Fig. 2c) evidences the statistical correlation between the occurrence of the three plateaus.

Given the observed high G values of such single-molecule junctions (reaching $0.8G_o$ in the TFc case) and their sequential correlation, we hypothesize that the molecular junction forms effective parallel electron pathways by bridging multiple Fc units at the same time (Fig. 3b). The different bridging configurations for BFc and TFc will be denoted by BFc_n and TFc_n, where *n* defines the number of Fc units effectively connected between the two electrodes (Fig. 3b). It is important to stress that *n* denotes the number of "plugged" Fc units only and that the order in which the Fc units disconnect during the pulling sequence might occur in a totally random fashion and so Fig. 3b represents one possible scenario only. Figure 3a shows that the formation of the three molecular junction configurations, namely TFc_3, TFc_2 and TFc_1, occurs statistically in a sequential fashion as the tip retracts while sequentially unplugging each of the three Fc units (Fig. 3b).[66,69,70] In support of this picture, the plateau length analysis of the break junction traces in Fig. 2 (see SI section 4) do not correlate with any relevant molecular length, thus reinforcing the sequential unplugging of the Fc units in the backbone, ruling out junction dynamics involving fully molecular lifting. With this picture in mind, Figure 3c summarizes the different conductance trends and the hypothesized molecular junction configurations that will be challenged in the last section by computational calculations.

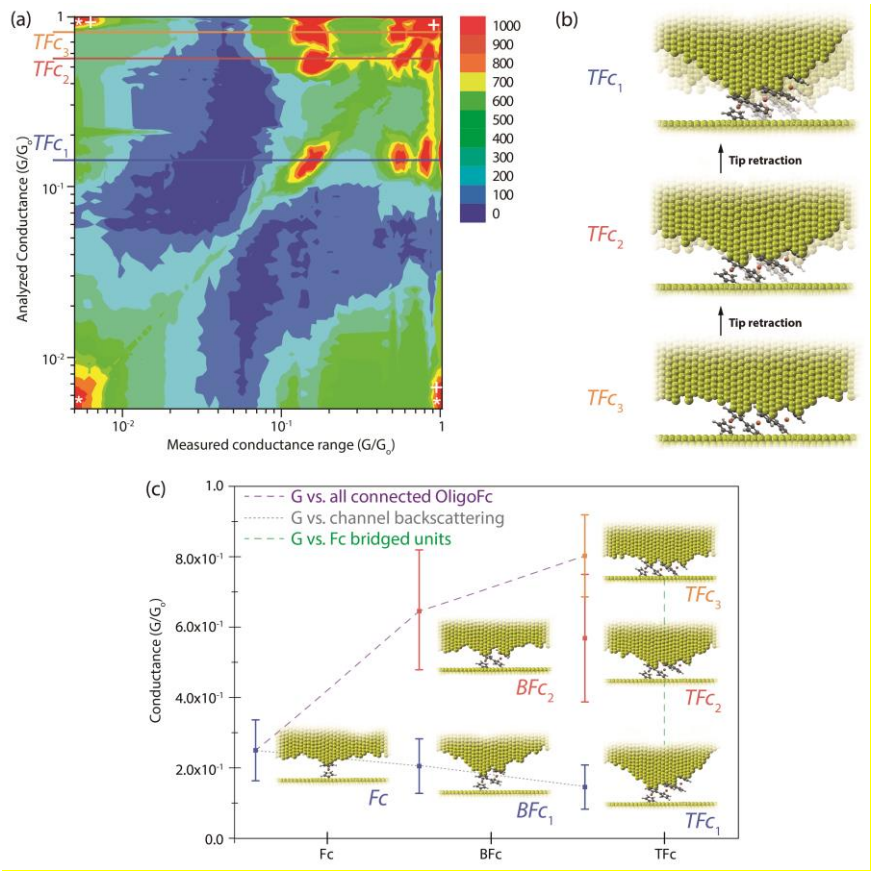

Fig. 3 (a) Logarithmic 2D cross-correlation conductance map of the individual traces for the TFc system. The horizontal lines are the selected conductance Bins that registered higher counting within the range of the three measured conductance plateaus for the TFc_3, TFc_2 and TFc_1 contact configurations (see Fig. 2 for notation). The three high-counts spots appearing in all three horizontal sections evidences the high sequential correlation of the three conductance events. The diagonal line reproduces the 1D conductance histograms of Fig. 2c. The high-counts spots labelled with an asterisk and a cross signs correspond to the background and saturation lines respectively, which are equally well correlated at the opposite corners of the map. **(b)** Cartoon representing the pulling sequence of a TFc molecular junction. As the STM tip is retracted, the initially bridged Fc units are sequentially disconnected from one of the electrodes terminals. **(c)** G values plot for the three oligoFc compounds and their different configurations are represented in cartoons insets.

Temperature-dependent single-molecule conductance

To determine the mechanism of charge transport through the Fc-based single-molecule wires, we measured their single-molecule conductance as a function of temperature *T*. Single-molecule transport experiments for Fc, BFc_1 and TFc_1 configurations with lower electrode-Fc connections were performed for varying *T*s from -10°C to 85°C (see also SI section 5). The Arrhenius plots (Fig. 4) of the averaged conductance values (*G* mean) show no significant dependence on *T* in all cases, indicating that the mechanism of charge transport is off-resonant tunneling for all wire contact configurations.[9,10]

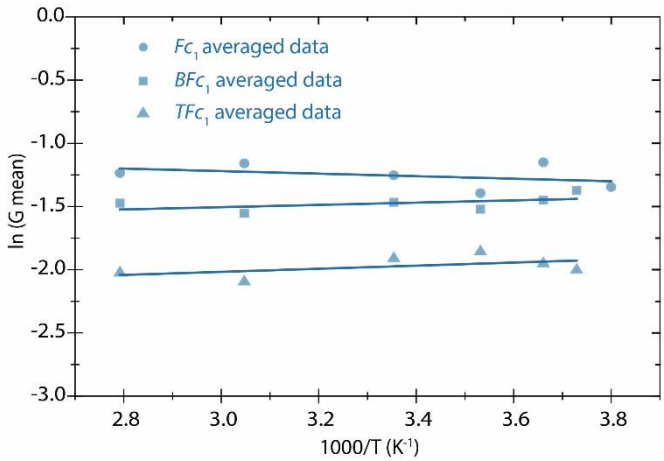

Fig. 4 Arrhenius plot of the Fc, BFc_1 and TFc_1 wires, representing the log of the average single-molecule conductance (G mean) versus the inverse of temperature. The applied voltage bias was set to 10 mV.

Tuning the energy of the oligoFc frontier orbital

We can fine-tune the high conductance values of the oligo-ferrocene wires by engineering the extension of the electronic coupling between the nearest Fc neighbors units, which, in turn, modulates the energy of the frontier orbital (see the next computational section) and so the molecular device conductance. As a probe of this concept, we synthesized a diferrocenyl compound, 1,4-diferrocenyl-1,3-butadiyne (BFc-butadiyne in Fig. 1, see SI section 1 for synthetic details), where two Fc units are electrically communicated through a conjugated butadiyne spacer. Figure 5b shows the single-molecule conductance values within the high conductance region near G_0 ($10^{-2}G_0$ to $1G_0$), which are dominated by two conductance maxima associated

with the two possible bridging configurations $(BFc\text{-}butadiyne)_1$ and $(BFc\text{-}butadiyne)_2$, following the same previous notation in Figure 2. Both $(BFc\text{-}butadiyne)_n$ configurations register lower conductance values, $0.08G_0$ and $0.23\ G_0$, than the BFc counterpart, where the Fc units are directly connected by a single C-C bond. The BFc-butadiyne junction gives us the opportunity to challenge the proposed junction geometry shown in Fig. 3b as follow: we have explored the lower G range ($10^{-3}G_0$-$10^{-2}G_0$) to seek for possible extended junction configurations (Fig. 5a inset) where the oligoFc wire is connected with the classical wiring picture through the distal Fc units[3]. To this aim, the low conductance region was analyzed for the BFc-butadiyne compound (Fig. 5a) whose side-to-side molecular conductance can be directly compared to the conductance values of the same butadiyne backbone previously measured using different anchoring chemistry.[71,72] The obtained value in 5a, $0.0034G_0$, is within the range of previously measured high conductance values of the same compound using pyridine as the anchoring units[71]. This result provides qualitative evidences that the conjugated spacer between the Fc units in the BFc-butadiyne dominates the charge transport in the low current range, thus reinforcing the proposed multi-contact configuration pictured within the higher G range. This result is also captured by the transmission calculations in next section.

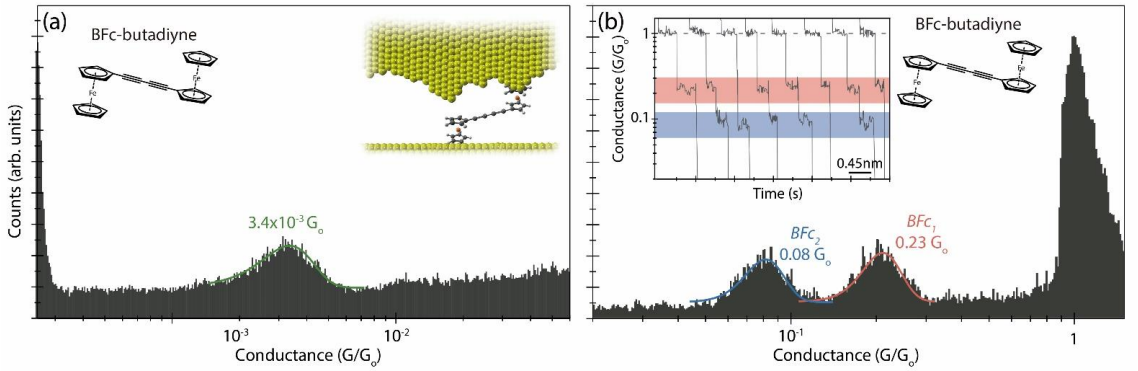

Fig. 5 Semi-log conductance histograms of BFc-butadiyne within the low range ($10^{-3}G_0$-$10^{-2}G_0$) **(a)** and high range ($10^{-2}G_0$ to $1G_0$) **(b)** of G. The conductance values are extracted from Gaussian fits of the peaks. The inset in (b) shows representative individual current traces displaying plateau features used to build the 1D histogram. The shadow coloured bands indicate the range of conductance for each plateau (line width extracted from the FWHM of the fitted histogram peaks). The applied voltage bias was set to 10 mV.

DFT-orbitals and transmission functions

Table I. HOMO-LUMO representations of the isosurface plots (isovalue = 0.03) and energies (in eV) for the four molecular systems (see SI section 6.2 for the full MO diagrams) calculated at the B3LYP/TZV level. Adjacent energy levels (lines below the MO representation) in the same compound denote MO degeneracy, while piled up levels are energetically separated MOs.

	HOMO		LUMO	
BFc-Butadiyne	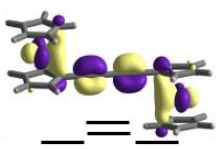	-5.40 eV -5.62 eV -5.65, -5.66 eV	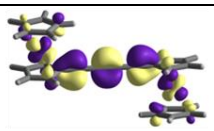	-1.36 eV

Fc	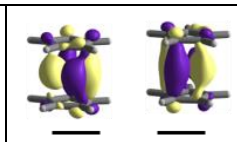	-5.44, -5.44 eV	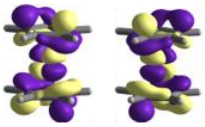	-0.488 eV
BFc	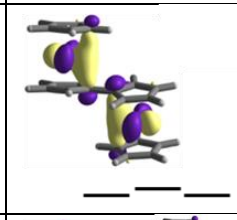	-5.28 eV -5.42, 5.43 eV	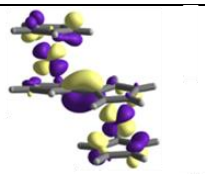	-0.742 eV
TFc	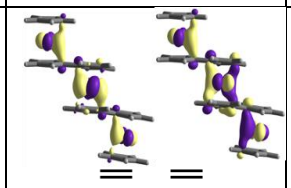	-5.25, -5.27 eV -5.42, -5.42 eV	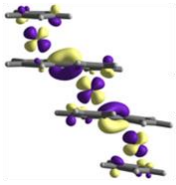	-0.833 eV

Table I visualizes the molecular orbitals for all studied compounds calculated using density functional theory (DFT) at the B3LYP/TZV level in the gas-phase (for details on the computational calculations see SI section 6). The HOMO levels correspond to quasi-degenerated MOs with high contributions from the metal d_{xy} and d_{x2-y2} orbitals that have a σ bonding interaction with the cyclopentadienyl (Cp) rings. A similar situation is found for the LUMO levels with the metal d_{xz} and d_{yz} orbitals that have also strong contribution of the Cp ligands with antibonding character. The computed HOMO energy (E_{HOMO}) trend along the Fc, BFc and TFc series (see Table I) correlates well with the high conductance features (all connected Fc units) in the histograms for the Fc, BFc_2, BFc-$butadiyne_2$ and TFc_3, and suggests the HOMO frontier orbital as the transport-relevant orbital due to its close proximity in energy to the Au Fermi energy (around -5 eV), also in agreement with previous works.[48,73–76] The correlation shows that by increasing the number of Fc units in the molecule, the E_{HOMO} level and its degree of degeneracy increase approaching the metal Fermi energy, thus decreasing the tunneling barrier height, $\delta E = E_{HOMO} - E_F$, which is in agreement with the increase in tunneling rate with increasing the oligoFc length (Fig. 3c, purple line). The DFT-computed frontier orbitals show an extended side-to-side delocalization of the HOMO in all cases (Table I). The saturating conductance behaviour going from the Fc to the all Fc-connected TFc is captured by the HOMO-Fermi level alignment (Fig. 6).

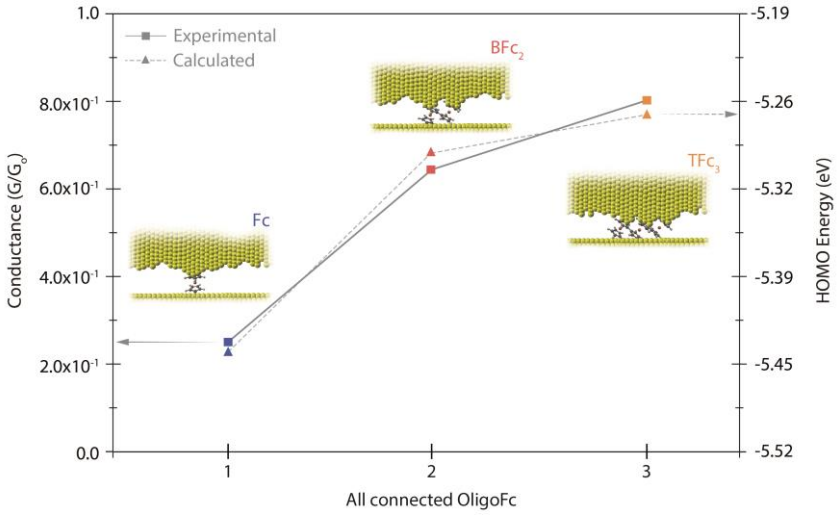

Fig. 6 Comparative trend between the experimental G and the DFT calculated HOMO energy for the Fc (1), BFc_2 (2) and TFc_3 (3) compounds.

We have also performed non-equilibrium Green function (NEGF) calculations combined with DFT approaches to calculate the conductance and the transmission functions (see Computational details in SI Section 6) for the three Fc, BFc, and TFc single-molecule junctions. We have employed a model structure for the junction with two gold hillocks flanking each Fc unit to simulate the STM scenario, where all Fc units are initially connected to both junction electrodes (Fig. 7a). To simulate the sequential Fc disconnection as we pull, two Au hillocks are removed, one at a time, from one side of each of the two Fc units, and the transmission function is recalculated for each case (Fig. 7b-c). This picture is not intended to capture the pulling dynamics taking place in the experiment, but it recreates the different expected molecular connections as the junction electrodes are being separated. Figures 7d-f show the corresponding transmission curves for the three cases. The calculated conductance is extracted from the integration of the transmission curve (Landauer equation) within the experimental bias energy window (at E=0 in Fig. 7d-f) assuming linear regime. Since GGA functionals with poor HOMO-LUMO gap determination are usually employed to obtain the transmission curves in periodic systems, the obtained functions in Figures 7d-f are merely used to extract the transmission values near the Fermi level E_F, with independence of whose tail, either HOMO or LUMO of the transmission function, has the largest contribution. For comparison, we have also considered a "flat electrodes" configuration where the oligoFc compound is trapped between two atomically flat surfaces (see Fig. S6.1 and S6.2). We recognize that such scenario would be much less realistic in a break-junction experiment, where a metallic quantum point contact breaks in every cycle (see the prominent 1 G_0 feature in Fig. 2). The obtained much lower values for the calculated transmission in this case also reinforce that and lead us to propose the "multiple-tips" scenario represented in Fig. 7a-c as the most plausible one.

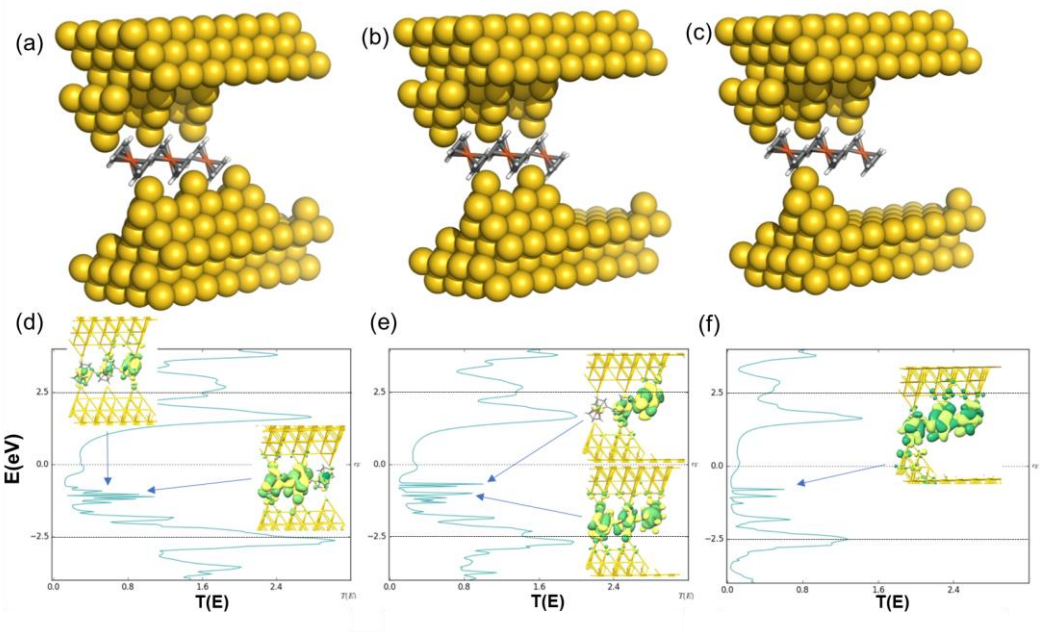

Fig. 7 Transmission curves (bottom panel) for the three different molecule/electrode contacts for the TFc molecule (top panel) calculated with the ATK code and PBE functional. The dotted line around the Fermi energy denotes the integrated G corresponding to the experimental bias window (tens of mVs). Transmissions higher than 1 originate from the contribution of several channels. Transmission eigenfunctions are plotted for some frontier orbitals. The transmission eigenstates are obtained by diagonalizing the transmission matrix and the corresponding eigenvalues indicate the importance of each eigenstate in transport. As it is a complex wavefunction, the color map represents the phase of the function from 0 to 2π by dark green to yellow colors. The threshold value employed for the isosurfaces is 0.3.

Figure 8 shows the correlation of the experimental single-molecule *G* values of the TFc compound (Figures 2c) with the calculated conductance values from the TFc transmission curves within the experimental bias windows for the cases with 1, 2 and 3 bridged Fc units. Again, the observed saturating conductance behaviour is captured by the NEGF-DFT calculations. Last, we have considered quantum interference effects given the existence of parallel pathways defined by each individually connected Fc unit in TFc_2 and TFc_3 as compared to previous work.[77] The transmission eigen states did not produce a clear interference trend among the possible Fc pathways. A possible explanation for this resides in the fact that the parallel pathways in our oligoFc junctions are independently connected to the electrodes.

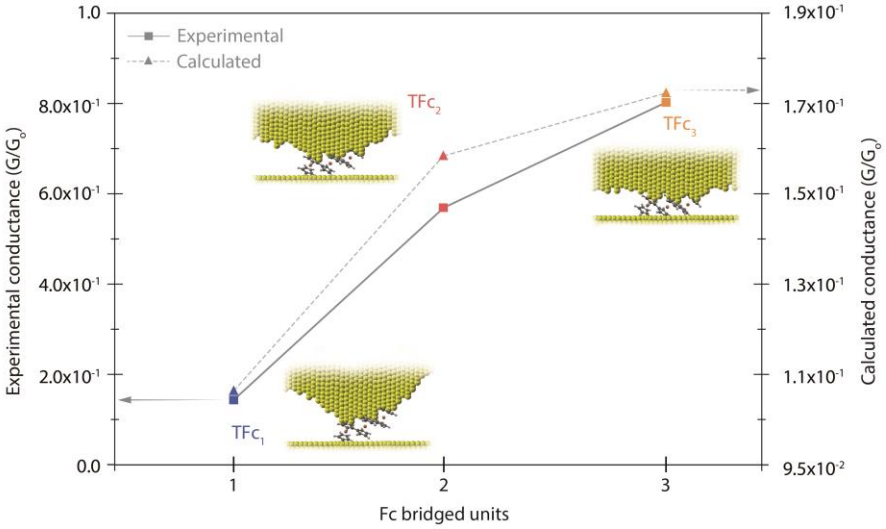

Fig. 8 Comparative trend between the experimental G and the calculated NEGF-DFT G values for the TFc_1, TFc_2 and TFc_3 contact configurations.

The last slight trend to be analysed from the overview Fig. 3c (grey line), can be qualitatively evaluated by plotting the transmission pathways for the two extreme cases: Fc and TFc_1 (Fig. 9). The direct comparison of the transmission pathways shows a better efficiency for the Fc system, as experimentally found, than for the TFc_1 case. In the latter, the lack of an effective connection through the two unbridged Fc units increases the backscattering effect in the incoming electron waves as compared to the former Fc case.

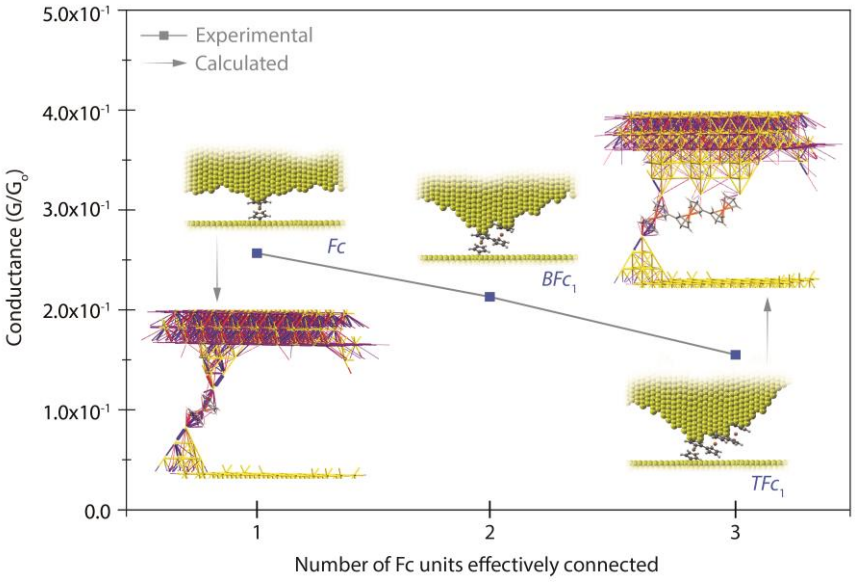

Fig. 9 Transmission pathways representation (large inset pictures) for the Fc and TFc_1 contacts. The colour of the arrows indicates the angle of the direction of the transport, blue (0°, forward) and red (180°, backward), respectively, and the intermediate colours (0-180°). The width of the arrow is related to the magnitude of the transport.

Conclusions

In conclusion, we have measured the single-molecule conductance of a series of Fc-oligomers (Fc, BFc and TFc), which efficiently couple to two metal leads in the absence of linker groups via connecting multiple Fc units in a simultaneous fashion. The result is a highly conductive molecular wire under coherent tunneling regime, whose conductance results in exceedingly high values of up to 0.8 G_o, near the ballistic conductance quantum, G_o. Our computed DFT orbitals show that the delocalized HOMO frontier orbital increases in energy and degeneracy in the order BFc-butadiyne<Fc<BFc<TFc, approaching the Au electrode Fermi energy and explaining the same increasing conductance trend for the configurations where all Fc units are connected. Moreover, the calculated transmission functions recreate the saturating conductance increase for each individual compound when a larger number of Fc units within the same backbone are being effectively bridged in the molecular junction.

Interestingly, this work shows that the Fc units can interact strongly with the electrodes of the STM break junction most likely via the distal uncoordinated atoms at the tips of the electrodes, as opposed to other Fc-based backbones where the Fc unit is isolated by axial linkers[44,46] or SAM-based junctions with the Fc units in van der Waals contact with the electrodes[6]. The consequence is that in the former, the molecular frontier orbitals delocalize resulting in a molecular junction displaying near ballistic transport with $G=0.8G_0$, *i.e*. the junctions are in the strong coupling regime, while in the latter the molecular frontier orbital are confined in the molecule resulting in a more resistive molecular junction. These observations suggest that the properties of these classes of junctions are very different due to differences in chemical reactivity between atomic tip-shaped and flat-like electrodes. Our work also exemplifies how the junction rupture dynamics can be exploited to control the number of molecule-electrode anchoring points sequentially by simply controlling the substrate-to-tip distance.

Overall, the results show a single-molecule wire displaying near-ballistic charge transport whose conductance can be modulated through the molecularly engineered extension of the Fc low-lying molecular orbital and the number of electrode/Fc contact points. This work also suggests the use of Fc as a new tunable molecule/electrode anchoring group with a simple contact configuration (single conductance signature) and a low energy tunneling barrier for charge injection.

Associated Content

Supporting Information

The Supporting Information is available free of charge on the ACS Publications website at DOI:

Synthetic details, technical details of the single-molecule transport, single-molecule conductance measurements in different solvents, 2D conductance and plateau length histograms, temperature-dependent single-molecule measurement, computational methods and additional calculations, and sample preparation.

Author Information

Corresponding Authors

*ismael.diez_perez@kcl.ac.uk

*christian.nijhuis@nus.edu.sg

*eliseo.ruiz@ub.edu

Acknowledgements

This research was supported by the MINECO Spanish national projects CTQ2015-71406-ERC, CTQ2015-64579-C3-1-P, CTQ2015-64579-C3-3-P (MINECO/FEDER, EU) and MDM-2017-0767. N.D. acknowledges ARC DECRA Fellowship DE160101101. S.C. acknowledges ARC DECRA Fellowship DE160100732. E. R. thanks Generalitat de Catalunya for an ICREA Academia award. I. D.-P. thanks Kings College London for startup support. We also acknowledge the Minister of Education (MOE) for supporting this research under award No. MOE2015-T2-2-134. Prime Minister's Office, Singapore under its Medium sized centre program is also acknowledged for supporting this research.

References

(1) Cuevas, J. C.; Scheer, E. FRONT MATTER. In *Molecular Electronics*; WORLD SCIENTIFIC, 2010; Vol. 1, pp i–xix.

(2) Okawa, Y.; Mandal, S. K.; Hu, C.; Tateyama, Y.; Goedecker, S.; Tsukamoto, S.; Hasegawa, T.; Gimzewski, J. K.; Aono, M. Chemical Wiring and Soldering toward All-Molecule Electronic Circuitry. *J. Am. Chem. Soc.* **2011**, *133* (21), 8227–8233.

(3) Xu, B.; Tao, N. J. Measurement of Single-Molecule Resistance by Repeated Formation of Molecular Junctions. *Science* **2003**, *301* (5637), 1221–1223.

(4) Song, H.; Kim, Y.; Jang, Y. H.; Jeong, H.; Reed, M. A.; Lee, T. Observation of Molecular Orbital Gating. *Nature* **2009**, *462* (7276), 1039–1043.

(5) Díez-Pérez, I.; Hihath, J.; Lee, Y.; Yu, L.; Adamska, L.; Kozhushner, M. a; Oleynik, I. I.; Tao, N. Rectification and Stability of a Single Molecular Diode with Controlled Orientation. *Nat. Chem.* **2009**, *1* (8), 635–641.

(6) Yuan, L.; Nerngchamnong, N.; Cao, L.; Hamoudi, H.; del Barco, E.; Roemer, M.; Sriramula, R. K.; Thompson, D.; Nijhuis, C. A. Controlling the Direction of Rectification in a Molecular Diode. *Nat. Commun.* **2015**, *6*, 6324.

(7) Wan, A.; Suchand Sangeeth, C. S.; Wang, L.; Yuan, L.; Jiang, L.; Nijhuis, C. A. Arrays of High Quality SAM-Based Junctions and Their Application in Molecular Diode Based Logic. *Nanoscale* **2015**, *7* (46), 19547–19556.

(8) Poot, M.; Osorio, E.; O'Neill, K.; Thijssen, J. M.; Vanmaekelbergh, D.; van Walree, C. A.; Jenneskens, L. W.; van der Zant, H. S. J. Temperature Dependence of Three-Terminal Molecular Junctions with Sulfur End-Functionalized Tercyclohexylidenes. *Nano Lett.* **2006**, *6* (5), 1031–1035.

(9) Engelkes, V. B.; Beebe, J. M.; Frisbie, C. D. Length-Dependent Transport in Molecular

Junctions Based on SAMs of Alkanethiols and Alkanedithiols: Effect of Metal Work Function and Applied Bias on Tunneling Efficiency and Contact Resistance. *J. Am. Chem. Soc.* **2004**, *126* (43), 14287–14296.

(10) Hines, T.; Diez-Perez, I.; Hihath, J.; Liu, H.; Wang, Z. S.; Zhao, J.; Zhou, G.; M??llen, K.; Tao, N. Transition from Tunneling to Hopping in Single Molecular Junctions by Measuring Length and Temperature Dependence. *J. Am. Chem. Soc.* **2010**, *132* (33), 11658–11664.

(11) Dell, E. J.; Capozzi, B.; Xia, J.; Venkataraman, L.; Campos, L. M. Molecular Length Dictates the Nature of Charge Carriers in Single-Molecule Junctions of Oxidized Oligothiophenes. *Nat. Chem.* **2015**, *7* (3), 209–214.

(12) Kaliginedi, V.; Moreno-García, P.; Valkenier, H.; Hong, W.; García-Suárez, V. M.; Buiter, P.; Otten, J. L. H.; Hummelen, J. C.; Lambert, C. J.; Wandlowski, T. Correlations between Molecular Structure and Single-Junction Conductance: A Case Study with Oligo(phenylene-Ethynylene)-Type Wires. *J. Am. Chem. Soc.* **2012**, *134* (11), 5262–5275.

(13) Diez-Perez, I.; Hihath, J.; Hines, T.; Wang, Z.-S.; Zhou, G.; Müllen, K.; Tao, N. Controlling Single-Molecule Conductance through Lateral Coupling of π Orbitals. *Nat. Nanotechnol.* **2011**, *6* (4), 226–231.

(14) Yamada, R.; Kumazawa, H.; Noutoshi, T.; Tanaka, S.; Tada, H. Electrical Conductance of Oligothiophene Molecular Wires. *Nano Lett.* **2008**, *8* (4), 1237–1240.

(15) Meisner, J. S.; Kamenetska, M.; Krikorian, M.; Steigerwald, M. L.; Venkataraman, L.; Nuckolls, C. A Single-Molecule Potentiometer. *Nano Lett.* **2011**, *11* (4), 1575–1579.

(16) Xu, B. Q.; Li, X. L.; Xiao, X. Y.; Sakaguchi, H.; Tao, N. J. Electromechanical and Conductance Switching Properties of Single Oligothiophene Molecules. *Nano Lett.* **2005**, *5* (7), 1491–1495.

(17) Venkataraman, L.; Park, Y. S.; Whalley, A. C.; Nuckolls, C.; Hybertsen, M. S.; Steigerwald, M. L. Electronics and Chemistry: Varying Single-Molecule Junction Conductance Using Chemical Substituents. *Nano Lett.* **2007**, *7* (2), 502–506.

(18) Aragonès, A. C.; Darwish, N.; Im, J.; Lim, B.; Choi, J.; Koo, S.; Díez-Pérez, I. Fine-Tuning of Single-Molecule Conductance by Tweaking Both Electronic Structure and Conformation of Side Substituents. *Chem. - A Eur. J. (Weinheim an der Bergstrasse, Ger.* **2015**, *21* (21), 7716–7720.

(19) Xiao, X.; Nagahara, L. A.; Rawlett, A. M.; Tao, N. Electrochemical Gate-Controlled Conductance of Single Oligo(phenylene Ethynylene)s. *J. Am. Chem. Soc.* **2005**, *127* (25), 9235–9240.

(20) Haiss, W.; van Zalinge, H.; Bethell, D.; Ulstrup, J.; Schiffrin, D. J.; Nichols, R. J. Thermal Gating of the Single Molecule Conductance of Alkanedithiols. *Faraday Discuss.* **2006**, *131*, 253–264.

(21) Venkataraman, L.; Klare, J. E.; Nuckolls, C.; Hybertsen, M. S.; Steigerwald, M. L. Dependence of Single-Molecule Junction Conductance on Molecular Conformation. *Nature* **2006**, *442* (7105), 904–907.

(22) Vonlanthen, D.; Mishchenko, A.; Elbing, M.; Neuburger, M.; Wandlowski, T.; Mayor, M. Chemically Controlled Conductivity: Torsion-Angle Dependence in a Single-Molecule Biphenyldithiol Junction. *Angew. Chemie Int. Ed.* **2009**, *48* (47), 8886–8890.

(23) Chen, F.; Tao, N. J. Electron Transport in Single Molecules: From Benzene to Graphene. *Acc. Chem. Res.* **2009**, *42* (3), 429–438.

(24) Zangmeister, C. D.; S. W. Robey; R. D. van Zee, A.; Kushmerick, J. G.; Naciri, J.; And, Y. Y.; Tour, J. M.; B. Varughese; B. Xu, A.; Reutt-Robey, J. E. Fermi Level Alignment in Self-Assembled Molecular Layers: The Effect of Coupling Chemistry. *J. Phys. Chem. B* **2006**, *110* (34), 17138–17144.

(25) Yuan, L.; Franco, C.; Crivillers, N.; Mas-Torrent, M.; Cao, L.; Sangeeth, C. S. S.; Rovira, C.; Veciana, J.; Nijhuis, C. A. Chemical Control over the Energy-Level Alignment in a Two-Terminal Junction. *Nat. Commun.* **2016**, *7*, 12066.

(26) Kim, B.; Beebe, J. M.; Jun, Y.; Zhu, X.-Y.; Frisbie, C. D. Correlation between HOMO Alignment and Contact Resistance in Molecular Junctions: Aromatic Thiols versus Aromatic Isocyanides. *J. Am. Chem. Soc.* **2006**, *128* (15), 4970–4971.

(27) Chen, W.; Li, H.; Widawsky, J. R.; Appayee, C.; Venkataraman, L.; Breslow, R. Aromaticity Decreases Single-Molecule Junction Conductance. *J. Am. Chem. Soc.* **2014**, *136* (3), 918–920.

(28) Chen, F.; Li, X.; Hihath, J.; Huang, Z.; Tao, N. Effect of Anchoring Groups on Single-Molecule Conductance: Comparative Study of Thiol-, Amine-, and Carboxylic-Acid-Terminated Molecules. *J. Am. Chem. Soc.* **2006**, *128* (49), 15874–15881.

(29) Park, Y. S.; Whalley, A. C.; Kamenetska, M.; Steigerwald, M. L.; Hybertsen, M. S.; Nuckolls, C.; Venkataraman, L. Contact Chemistry and Single-Molecule Conductance: A Comparison of Phosphines, Methyl Sulfides, and Amines. *J. Am. Chem. Soc.* **2007**, *129* (51), 15768–15769.

(30) Hong, W.; Manrique, D. Z.; Moreno-García, P.; Gulcur, M.; Mishchenko, A.; Lambert, C. J.; Bryce, M. R.; Wandlowski, T. Single Molecular Conductance of Tolanes: Experimental and Theoretical Study on the Junction Evolution Dependent on the Anchoring Group. *J. Am. Chem. Soc.* **2012**, *134* (4), 2292–2304.

(31) Zotti, L. A.; Kirchner, T.; Cuevas, J.-C.; Pauly, F.; Huhn, T.; Scheer, E.; Erbe, A. Revealing the Role of Anchoring Groups in the Electrical Conduction Through Single-Molecule Junctions. *Small* **2010**, *6* (14), 1529–1535.

(32) KEALY, T. J.; PAUSON, P. L. A New Type of Organo-Iron Compound. *Nature* **1951**, *168* (4285), 1039–1040.

(33) Dou, R. F.; Zhong, D. Y.; Wang, W. C.; Wedeking, K.; Erker, G.; Chi, L.; Fuchs, H. Structures and Stability of Ferrocene Derivative Monolayers on Ag(110): Scanning Tunneling Microscopy Study. *J. Phys. Chem. C* **2007**, *111* (33), 12139–12144.

(34) Yuan, L.; Breuer, R.; Jiang, L.; Schmittel, M.; Nijhuis, C. A. A Molecular Diode with a Statistically Robust Rectification Ratio of Three Orders of Magnitude. *Nano Lett.* **2015**, *15* (8), 5506–5512.

(35) Waldfried, C.; Welipitiya, D.; Hutchings, C. W.; de Silva, H. S. V.; Gallup, G. A.; Dowben, P. A.; Pai, W. W.; Zhang, J.; Wendelken, J. F.; Boag, N. M. Preferential Bonding Orientations of Ferrocene on Surfaces. *J. Phys. Chem. B* **1997**, *101* (47), 9782–9789.

(36) Heinrich, B. W.; Limot, L.; Rastei, M. V; Iacovita, C.; Bucher, J. P.; Djimbi, D. M.; Massobrio, C.; Boero, M. Dispersion and Localization of Electronic States at a ferrocene/Cu(111) Interface. *Phys. Rev. Lett.* **2011**, *107* (21), 216801.

(37) Morari, C.; Rungger, I.; Rocha, A. R.; Sanvito, S.; Melinte, S.; Rignanese, G.-M. Electronic Transport Properties of 1,1'-Ferrocene Dicarboxylic Acid Linked to Al(111) Electrodes. *ACS Nano* **2009**, *3* (12), 4137–4143.

(38) Dowben, P. .; Waldfried, C.; Komesu, T.; Welipitiya, D.; McAvoy, T.; Vescovo, E. The Occupied and Unoccupied Electronic Structure of Adsorbed Ferrocene. *Chem. Phys. Lett.* **1998**, *283* (1–2), 44–50.

(39) Quardokus, R. C.; Wasio, N. A.; Forrest, R. P.; Lent, C. S.; Corcelli, S. A.; Christie, J. A.; Henderson, K. W.; Kandel, S. A. Adsorption of Diferrocenylacetylene on Au(111) Studied by Scanning Tunneling Microscopy. *Phys. Chem. Chem. Phys.* **2013**, *15* (18), 6973–6981.

(40) Ormaza, M.; Abufager, P.; Bachellier, N.; Robles, R.; Verot, M.; Le Bahers, T.; Bocquet, M.-L.; Lorente, N.; Limot, L. Assembly of Ferrocene Molecules on Metal Surfaces Revisited. *J. Phys. Chem. Lett.* **2015**, *6* (3), 395–400.

(41) Welipitiya, D.; Dowben, P. A.; Zhang, J.; Pai, W. W.; Wendelken, J. F. The Adsorption and Desorption of Ferrocene on Ag(100). *Surf. Sci.* **1996**, *367* (1), 20–32.

(42) Woodbridge, C. M.; Pugmire, D. L.; Johnson, R. C.; Boag, N. M.; Langell, M. A. HREELS and XPS Studies of Ferrocene on Ag(100) †. *J. Phys. Chem. B* **2000**, *104* (14), 3085–3093.

(43) Xiao, X.; Brune, D.; He, J.; Lindsay, S.; Gorman, C. B.; Tao, N. Redox-Gated Electron Transport in Electrically Wired Ferrocene Molecules. *Chem. Phys.* **2006**, *326* (1), 138–143.

(44) Getty, S.; Engtrakul, C.; Wang, L.; Liu, R.; Ke, S.-H.; Baranger, H.; Yang, W.; Fuhrer, M.; Sita, L. Near-Perfect Conduction through a Ferrocene-Based Molecular Wire. *Phys. Rev. B* **2005**, *71* (24), 241401.

(45) Lu, Q.; Yao, C.; Wang, X.; Wang, F. Enhancing Molecular Conductance of Oligo(P -Phenylene Ethynylene)s by Incorporating Ferrocene into Their Backbones. *J. Phys. Chem. C* **2012**, *116* (33), 17853–17861.

(46) Sun, Y.-Y.; Peng, Z.-L.; Hou, R.; Liang, J.-H.; Zheng, J.-F.; Zhou, X.-Y.; Zhou, X.-S.; Jin, S.; Niu, Z.-J.; Mao, B.-W. Enhancing Electron Transport in Molecular Wires by Insertion of a Ferrocene Center. *Phys. Chem. Chem. Phys. Phys. Chem. Chem. Phys* **2260**, *16* (16), 2260–2267.

(47) He, J.; Lindsay, S. M. On the Mechanism of Negative Differential Resistance in Ferrocenylundecanethiol Self-Assembled Monolayers. *J. Am. Chem. Soc.* **2005**, *127* (34), 11932–11933.

(48) Nijhuis, C. A.; Reus, W. F.; Whitesides, G. M. Mechanism of Rectification in Tunneling Junctions Based on Molecules with Asymmetric Potential Drops. *J. Am. Chem. Soc.* **2010**, *132* (51), 18386–18401.

(49) Gidron, O.; Diskin-Posner, Y.; Bendikov, M. High Charge Delocalization and Conjugation in Oligofuran Molecular Wires. *Chemistry* **2013**, *19* (39), 13140–13150.

(50) Aguirre-Etcheverry, P.; O'Hare, D. Electronic Communication through Unsaturated Hydrocarbon Bridges in Homobimetallic Organometallic Complexes. *Chem. Rev.* **2010**, *110* (8), 4839–4864.

(51) Leatherman, G.; Durantini, E. N.; Gust, D.; Moore, T. A.; Moore, A. L.; Stone, S.; Zhou, Z.; Rez, P.; Liu, Y. Z.; Lindsay, S. M. Carotene as a Molecular Wire: Conducting Atomic Force Microscopy. *J. Phys. Chem. B* **1999**, *103* (20), 4006–4010.

(52) Simeone, F. C.; Yoon, H. J.; Thuo, M. M.; Barber, J. R.; Smith, B.; Whitesides, G. M. Defining the Value of Injection Current and Effective Electrical Contact Area for EGaIn-Based Molecular Tunneling Junctions. *J. Am. Chem. Soc.* **2013**, *135* (48), 18131–18144.

(53) Sangeeth, C. S. S.; Demissie, A. T.; Yuan, L.; Wang, T.; Frisbie, C. D.; Nijhuis, C. A. Comparison of DC and AC Transport in 1.5–7.5 Nm Oligophenylene Imine Molecular Wires across Two Junction Platforms: Eutectic Ga–In versus Conducting Probe Atomic Force Microscope Junctions. *J. Am. Chem. Soc.* **2016**, *138* (23), 7305–7314.

(54) Amdursky, N.; Marchak, D.; Sepunaru, L.; Pecht, I.; Sheves, M.; Cahen, D. Electronic Transport via Proteins. *Adv. Mater.* **2014**, *26* (42), 7142–7161.

(55) Yoshida, K.; Pobelov, I. V; Manrique, D. Z.; Pope, T.; Mészáros, G.; Gulcur, M.; Bryce, M. R.; Lambert, C. J.; Wandlowski, T. Correlation of Breaking Forces, Conductances and Geometries of Molecular Junctions. *Sci. Rep.* **2015**, *5*, 9002.

(56) Thompson, D.; Liao, J.; Nolan, M.; Quinn, A. J.; Nijhuis, C. A.; O'Dwyer, C.; Nirmalraj, P. N.; Schönenberger, C.; Calame, M. Formation Mechanism of Metal–Molecule–Metal Junctions: Molecule-Assisted Migration on Metal Defects. *J. Phys. Chem. C* **2015**, *119* (33), 19438–19451.

(57) Inkpen, M. S.; Lemmer, M.; Fitzpatrick, N.; Milan, D. C.; Nichols, R. J.; Long, N. J.; Albrecht, T. New Insights into Single-Molecule Junctions Using a Robust, Unsupervised Approach to Data Collection and Analysis. *J. Am. Chem. Soc.* **2015**, *137* (31), 9971–9981.

(58) Hines, T.; Díez-Pérez, I.; Nakamura, H.; Shimazaki, T.; Asai, Y.; Tao, N. Controlling Formation of Single-Molecule Junctions by Electrochemical Reduction of Diazonium Terminal Groups. *J. Am. Chem. Soc.* **2013**, *135* (9), 3319–3322.

(59) Aragonès, A. C. A. C.; Aravena, D.; Cerdá, J. I. J. I.; Acís-Castillo, Z.; Li, H.; Real, J. A. J. A.; Sanz, F.; Hihath, J.; Ruiz, E.; Díez-Pérez, I. Large Conductance Switching in a Single-Molecule Device through Room Temperature Spin-Dependent Transport. *Nano Lett.* **2016**, *16* (1), 218–226.

(60) Afsari, S.; Li, Z.; Borguet, E. Orientation-Controlled Single-Molecule Junctions. *Angew. Chemie Int. Ed.* **2014**, *53* (37), 9771–9774.

(61) Müller, K.-H. Effect of the Atomic Configuration of Gold Electrodes on the Electrical Conduction of Alkanedithiol Molecules. *Phys. Rev. B* **2006**, *73* (4), 45403.

(62) Ishizuka, K.; Suzuki, M.; Fujii, S.; Takayama, Y.; Sato, F.; Fujihira, M. Effect of Molecule–Electrode Contacts on Single-Molecule Conductivity of π-Conjugated System Measured by Scanning Tunneling Microscopy under Ultrahigh Vacuum. *Jpn. J. Appl. Phys.* **2006**, *45* (3B), 2037–2040.

(63) Li, C.; Pobelov, I.; Wandlowski, T.; Bagrets, A.; Arnold, A.; Evers, F. Charge Transport in Single Au | Alkanedithiol | Au Junctions: Coordination Geometries and Conformational Degrees of Freedom. *J. Am. Chem. Soc.* **2008**, *130* (1), 318–326.

(64) Li, X.; He, J.; Hihath, J.; Xu, B.; Lindsay, S. M.; Tao, N. Conductance of Single Alkanedithiols: Conduction Mechanism and Effect of Molecule-Electrode Contacts. *J. Am. Chem. Soc.* **2006**, *128* (6), 2135–2141.

(65) Moreno-García, P.; La Rosa, A.; Kolivoška, V.; Bermejo, D.; Hong, W.; Yoshida, K.; Baghernejad, M.; Filippone, S.; Broekmann, P.; Wandlowski, T.; et al. Charge Transport in C60-Based Dumbbell-Type Molecules: Mechanically Induced Switching between Two Distinct Conductance States. *J. Am. Chem. Soc.* **2015**, *137* (6), 2318–2327.

(66) Kiguchi, M.; Ohto, T.; Fujii, S.; Sugiyasu, K.; Nakajima, S.; Takeuchi, M.; Nakamura, H. Single Molecular Resistive Switch Obtained via Sliding Multiple Anchoring Points and Varying Effective Wire Length. *J. Am. Chem. Soc.* **2014**, *136* (20), 7327–7332.

(67) Mishchenko, A.; Zotti, L. A.; Vonlanthen, D.; Bürkle, M.; Pauly, F.; Cuevas, J. C.; Mayor, M.; Wandlowski, T. Single-Molecule Junctions Based on Nitrile-Terminated Biphenyls: A Promising New Anchoring Group. *J. Am. Chem. Soc.* **2011**, *133* (2), 184–187.

(68) Makk, P.; Tomaszewski, D.; Martinek, J.; Balogh, Z.; Csonka, S.; Wawrzyniak, M.; Frei, M.; Venkataraman, L.; Halbritter, A. Correlation Analysis of Atomic and Single-Molecule Junction Conductance. *ACS Nano* **2012**, *6* (4), 3411–3423.

(69) Miguel, D.; Álvarez de Cienfuegos, L.; Martín-Lasanta, A.; Morcillo, S. P.; Zotti, L. A.; Leary, E.; Bürkle, M.; Asai, Y.; Jurado, R.; Cárdenas, D. J.; et al. Toward Multiple Conductance Pathways with Heterocycle-Based Oligo(phenyleneethynylene) Derivatives. *J. Am. Chem. Soc.* **2015**, *137* (43), 13818–13826.

(70) Schneebeli, S. T.; Kamenetska, M.; Cheng, Z.; Skouta, R.; Friesner, R. a.; Venkataraman, L.; Breslow, R. Single-Molecule Conductance through Multiple π-π-Stacked Benzene Rings Determined with Direct Electrode-to-Benzene Ring Connections. *J. Am. Chem. Soc.* **2011**, *133* (7), 2136–2139.

(71) Wang, C.; Batsanov, A. S.; Bryce, M. R.; Martín, S.; Nichols, R. J.; Higgins, S. J.; García-Suárez, V. M.; Lambert, C. J. Oligoyne Single Molecule Wires. *J. Am. Chem. Soc.* **2009**, *131* (43), 15647–15654.

(72) Milan, D. C.; Al-Owaedi, O. A.; Oerthel, M.-C.; Marqués-González, S.; Brooke, R. J.; Bryce, M. R.; Cea, P.; Ferrer, J.; Higgins, S. J.; Lambert, C. J.; et al. Solvent Dependence of the Single Molecule Conductance of Oligoyne-Based Molecular Wires. *J. Phys. Chem. C* **2016**, *120* (29), 15666–15674.

(73) Lima, F. C. D. A.; Calzolari, A.; Caldas, M. J.; Iost, R. M.; Crespilho, F. N.; Petrilli, H. M. Electronic Structure of Self-Assembled Monolayers Modified with Ferrocene on a Gold Surface: Evidence of Electron Tunneling. *J. Phys. Chem. C* **2014**, *118* (40), 23111–23116.

(74) Lee, S. U.; Belosludov, R. V.; Mizuseki, H.; Kawazoe, Y. Control of Electron Transport by Manipulating the Conjugated Framework. *J. Phys. Chem. C* **2007**, *111* (42), 15397–15403.

(75) Bredow, T.; Tegenkamp, C.; Pfnür, H.; Meyer, J.; Maslyuk, V. V; Mertig, I. Ferrocene-1,1'-dithiol as Molecular Wire between Ag Electrodes: The Role of Surface Defects. *J. Chem. Phys.* **2008**, *128* (6), 64704.

(76) Jeong, H.; Kim, D.; Wang, G.; Park, S.; Lee, H.; Cho, K.; Hwang, W.-T.; Yoon, M.-H.; Jang, Y. H.; Song, H.; et al. Redox-Induced Asymmetric Electrical Characteristics of Ferrocene-Alkanethiolate Molecular Devices on Rigid and Flexible Substrates. *Adv. Funct. Mater.* **2014**, *24* (17), 2472–2480.

(77) VazquezH; SkoutaR; SchneebeliS; KamenetskaM; BreslowR; VenkataramanL; HybertsenM.S. Probing the Conductance Superposition Law in Single-Molecule Circuits with Parallel Paths. *Nat Nano* **2012**, *7* (10), 663–667.

Table of Contents (TOC) graphic